Nov 7th, 12:00 AM - Nov 8th, 12:00 AM

Web Bearing Capacity of Cold-Formed Ferritic Stainless Steel Unlipped Channels with Web perforations under the End-Two-Flange (ETF) Loading

Amir M. Yousefi

James B. P. Lim

G. Charles Clifton

Wei-Wen Yu International Specialty Conference on Cold-Formed Steel Structures
St. Louis, Missouri, U.S.A., November 7 & 8, 2018

Web Bearing Capacity of Cold-Formed Ferritic Stainless Steel Unlipped Channels With Web perforations Under the End-Two-Flange (ETF) Loading

Amir M. Yousefi[1a], James B.P. Lim*[1], G. Charles Clifton[1b]

[a] PhD scholar, Email: amirmohammad.yousefi@auckland.ac.nz

*Associate professor, E-mail: james.lim@auckland.ac.nz

[b] Associate Professor, E-mail: c.clifton@auckland.ac.nz

Abstract

Laboratory and numerical evaluations on the web bearing capacity of unlipped cold-formed ferritic stainless steel channels are described in this paper. The channels considered have circular perforations in the web and are loaded under the end-two-flange (ETF) load case. A total of 387 results comprising 27 laboratory and 360 numerical results are presented. A nonlinear quasi-static finite element (FE) model was developed for the numerical investigation. An extensive parametric study is described to determine web bearing capacity reduction factors for different sizes of circular web perforations and cross-section dimensions; the circular web perforations are either centred or offset to the load and reaction plates. It is noted that no cold-formed stainless steel standard provides capacity reduction factors for any end-two-flange load case. The capacity reduction factor equations are first compared to reduction factors previously recommended for lipped cold-formed stainless steel channels. It is found that these existing equations are unreliable and unconservative for unlipped channels by as much as 11%. From both laboratory and finite element results, web bearing capacity design equations are proposed for both sections, with and without web perforations.

Keywords: Cold-formed ferritic stainless steel; Unlipped channels; Finite element analysis; Web bearing capacity; Web perforation.

1 Introduction

In recent decades, the application of cold-formed stainless steel structural sections in industry have become increasingly prevalent worldwide due to their favourable material characteristics, notable corrosion and heat resistance, recycling options and aesthetic appeal. Among the all stainless steel material grades, ferritic stainless steel offers a competitive economical solution as cheaper alloys with little or no nickel content (Cashell and Baddoo 2014). To provide ease of access for services, the use of web perforations for secondary structural members are also becoming popular in industry (Lawson et al. 2015). Such web perforations, however, lead to sections being at more risk to localised failure in the web, particularly under transverse concentrated loads in the vicinity of the perforations; the failure is also influenced by the position of the perforations. This phenomenon is called web bearing failure, is also known as web crippling failure. The generic single or double track deflection

[1]Department of Civil and Environmental Engineering, The University of Auckland, New Zealand

track is a common application for web bearing failure where the flanges are not restrained. As an example, in industrial roofing where channel-sections are used as purlins located between the roofing and the rafter.

The concern of this research is to evaluate the web bearing capacity of unlipped cold-formed ferritic stainless steel channels having circular perforations in web; the channels are subject to the ETF load case. Design guidance recommended for cold-formed stainless steel structural members are presented in the ASCE Specification SEI/ASCE-8 (ASCE 2002), the Australian/New Zealand Standard AS/NZS 4673 (AS/NZS 2001) and the European Code Design of Steel Structures EN 1993-1-4 (CEN 2006) (which refers to EN 1993-1-3 (CEN 2006) for carbon steel). None of the aforementioned specifications, however, provide design guidance in regard to cold-formed stainless steel channels having perforations in web. Only the American Iron and Steel Institute Specification AISI S100 (AISI 2016) for cold-formed carbon steel provides reduction factors for determining the web bearing capacity of C-section webs; and this is only subject to one-flange loading. Furthermore, for the web bearing capacity of cold-formed stainless steel channels, SEI/ASCE-8 (ASCE 2002), AS/NZS 4673 (AS/NZS 2001) and EN 1993-1-4 (CEN 2006) make no distinction between lipped and unlipped flanges or to the different stainless steel grades. Again, only AISI S100 (AISI 2016) for cold-formed carbon steel structural members provides separate equations for lipped and unlipped flanges.

In the literature, no laboratory tests have been reported for unlipped cold-formed ferritic stainless steel channels having perforations in web subject to two-flange loading. For stainless steel lipped channels, Krovink and van den Berg (1994) and Krovink *et al.* (1995) have considered lipped cold-formed stainless steel channels subject to one-flange loading. Zhou and Young (2013; 2007a,b) considered the web bearing capacity of cold-formed stainless steel tubular sections, again without perforations. Research by Lawson *et al.* (2015), while concerned with circular web perforations, focussed on the bending capacity of the sections and not on the web bearing capacity under concentrated loads. Zhou and Young (2010) carried out a number of test programmes alongside numerical simulation on the web bearing capacity of aluminium hollow square sections having circular web perforation. The Authors have also recently conducted numerical studies on lipped cold-formed stainless steel channels having circular web perforations (Yousefi et al. 2017a,b,c, 2016a,b).Uunlipped channels only under two-flange loadings have also been tested by Yousefi et al. 2017d,e,f). In regards to cold-formed carbon steel, Lian et al. (2017; 2016) and Uzzaman et al. (2012; 2013) have tested lipped channels subject to one and two-flange loading (see Fig. 1).

This research describes a comprehensive laboratory and numerical study to determine the web bearing capacity of unlipped cold-formed ferritic stainless steel channels subject to ETF load case, as demonstrated in Figs. 2 and 3. Both cases of unlipped channels without and with circular web perforations are considered. Quasi-static finite element analyses (FEA) are then employed using the general application software ABAQUS (2014) to verify the numerical models against laboratory data. A good match between the laboratory and FE results has been attained. The developed FE model has then been used so to carry out an extensive parametric study to determine the capacity of unlipped channels having different web perforation sizes, load and reaction plates lengths and position of perforations in the web, as well as to assess the accuracy of existing design guidance presented in SEI/ASCE-8 (ASCE 2002), AS/NZS 4673 (AS/NZS 2001) and EN EN 1993-1-4 (CEN 2006). Using laboratory and finite element results, web bearing design equations are then proposed.

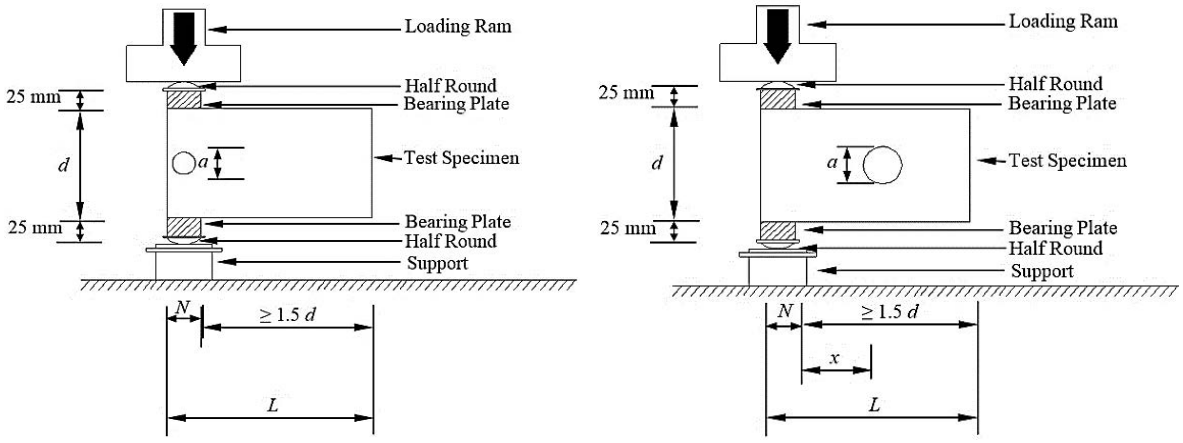

Figure 1: End-two-flange (ETF) loading condition after Uzzaman et al. (2013); (a) Centred web perforation, (b) Offset web perforation

2 Experimental investigation and finite element modelling

In total, 27 unlipped channels having either circular web perforation or without web perforation were considered. The ferritic stainless steel sheets (grade G430) were cut and press-braked to form unlipped channels for experimental study. In both cases, unlipped channels had three different depth sizes from 175mm to 250mm with web slenderness ratio (h/t) between 148.92 and 232.63. The channels length (L) were chosen from the AISI S100 Specification (AISI 2016) where length equals 1.5 times height of the sections, plus length of the load or reaction plates. For channels with circular perforation in web, diameter (a) was between 68mm to 100mm. The cross-section dimensions measured in the lab as well as notations for determining the parameters are shown in Table 1 and Fig. 2 respectively. Fig. 3 presents the web crippling test-setup under ETF load case. As can be seen in Fig. 3, the circular perforations were either in one end of the unlipped sections in between the load and reaction plates or in mid-length of the sections. The unlipped sections are under exterior/external two flange load case where concentrated transverse load applies at the end of the unlipped channels.

The sections have been coded so that the nominal section dimension, the length of the load or reaction plates and Web perforations ratio (A) can be determined from the coding system. As an example, the label "175-N100-A0.2" can be explained as follows. The first annotation is the nominal sections depth in millimeters. The annotation "N100" indicates the load or reaction plates length in millimeters (i.e. 100 mm). The Web perforations ratio (A) are defined as measured depth of the web perforations (a) over the measured depth of the plain part of the web (h) and can be one of 0.2, 0.4, 0.6 and 0.8; for example "A0.4" indicates a/h = 0.4. Unlipped sections without circular web perforations are indicated by "A0". Also, the letter "M" indicates web perforations located in between the load and reaction plates and the letter "O" indicates that the web perforations are in mid-length of the sections. The same definitions were used in the numerical investigation. Comparative hot-rolled steel stress strain curves can be found in Yousefi *et al.* (2014) and Rezvani *et al*. (2015).

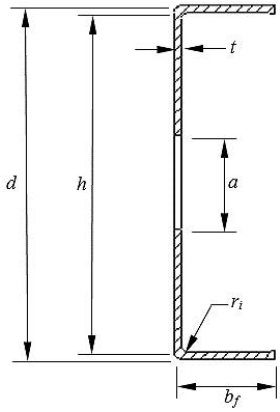

Figure 2: Definition of symbols

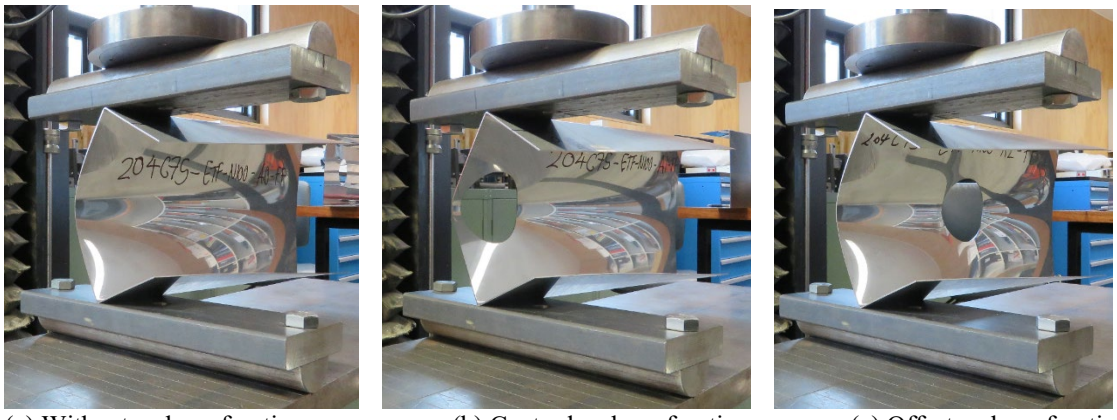

(a) Without web perforation (b) Centred web perforation (c) Offset web perforation

Figure 3: Experimental analysis of cold-formed steel channel sections under ETF loading condition

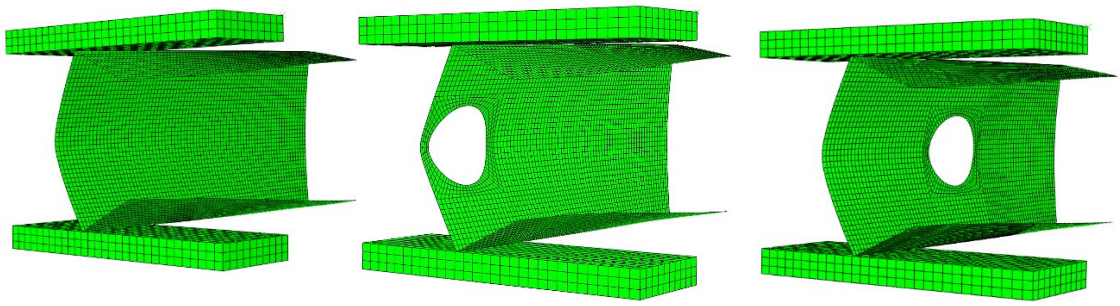

(a) Without web perforation (b) Centred web perforation (c) Offset web perforation

Figure 4: Numerical analysis of cold-formed steel channel sections under ETF loading condition

In this paper, finite element (FE) models are also developed using the general application software ABAQUS (2014) for the numerical investigation and the results presented in the parametric study. In previous study (2017c), static general models were used. Hence, nonlinear quasi-static models were used in this study as it was found that the elastic stiffness branch and post-buckling behaviour were better matched with the laboratory results; the ultimate loads, however, are generally unaffected. Fig. 4 shows the full scale of laboratory test set-up modelled in the numerical study. The typical finite element mesh of the unlipped channels as well as load and reaction plates are shown in Fig. 4. Finite element mesh sizes of 8 × 8 mm were used for the load and reaction plates and 5 × 5 mm for the unlipped channels. At least five elements were used for meshing the corner region of the channels due to transferring transverse loads from flanges to web. For modelling unlipped channels with web perforations, structured mesh with at least five elements was applied around the web perforations.

The laboratory and the finite element (FE) results were compared to determine the suitability of the models. The obtained results from web bearing test ultimate loads per single web (P_{Lab}) and the web bearing FEA ultimate loads per single web (P_{FEA}) are presented in Table 1. It is clear from Table 1 that the mean ratio of the laboratory results over FE results stances 1.00 having the coefficient of variation of COV=0.01. Overall, 3% was the maximum difference for the section 250x100-t1.2-N100-MA0.4 obtained from the FE and laboratory results. Fig. 5 presents the comparison of the load-displacement responses for section 200×65-t1.2-N100 for unlipped channels without and with perforations in web. A good agreement has been attained for both sections without and with perforations in web.

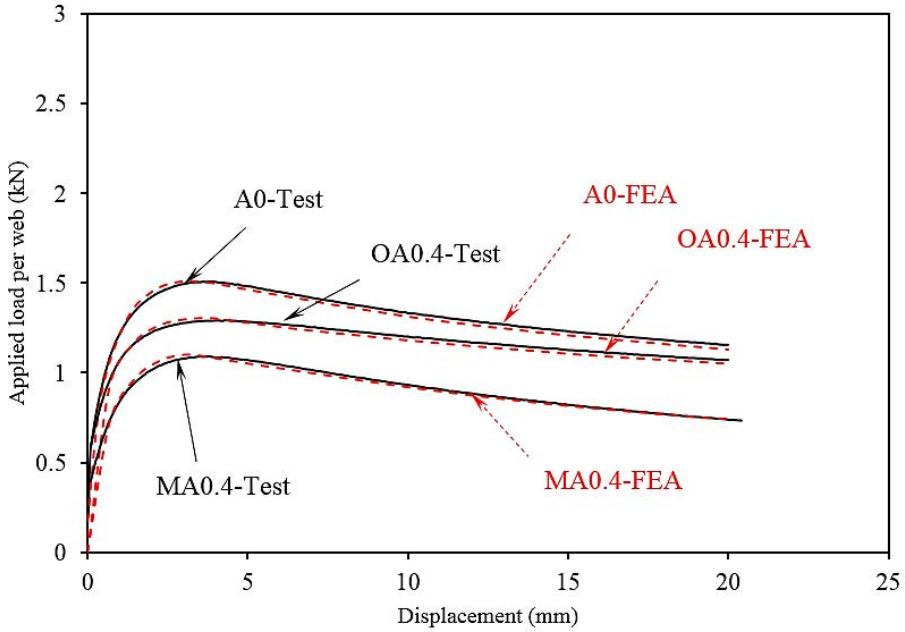

Figure 5: Comparison of web deformation curves for section 200×65-t1.2-N100

Table 1 Web bearing capacity comparison from laboratory and finite element analysis results

Section	Web slenderness ratio (h/t)	Web perforation ratio (a/h)	Lab. load per single web P_{LAB}(kN)	Web bearing capacity per single web predicted from FEA P_{FEA}(kN)	Comparison P_{LAB}/P_{FEA}
175x60-t1.2-N50-A0	150.55	0.00	1.51	1.53	0.99
175x60-t1.2-N50-MA0.4	154.53	0.39	0.99	0.98	1.01
175x60-t1.2-N50-OA0.4	151.63	0.39	1.29	1.29	1.00
175x60-t1.2-N75-A0	154.17	0.00	1.63	1.62	1.01
175x60-t1.2-N75-MA0.4	148.92	0.39	1.25	1.23	1.02
175x60-t1.2-N75-OA0.4	153.04	0.39	1.43	1.44	0.99
175x60-t1.2-N100-A0	155.70	0.00	1.76	1.76	1.00
175x60-t1.2-N100-MA0.4	153.10	0.39	1.33	1.32	1.01
175x60-t1.2-N100-OA0.4	154.46	0.39	1.57	1.59	0.99
200x75-t1.2-N50-A0	171.91	0.00	1.39	1.38	1.01
200x75-t1.2-N50-MA0.4	169.06	0.39	0.97	0.97	1.00
200x75-t1.2-N50-OA0.4	173.42	0.39	1.16	1.15	1.01
200x75-t1.2-N75-A0	171.93	0.00	1.44	1.46	0.99
200x75-t1.2-N75-MA0.4	200.97	0.39	0.99	1.00	0.99
200x75-t1.2-N75-OA0.4	176.39	0.39	1.23	1.24	0.99
200x75-t1.2-N100-A0	179.79	0.00	1.51	1.51	1.00
200x75-t1.2-N100-MA0.4	178.09	0.39	1.09	1.08	1.01
200x75-t1.2-N100-OA0.4	181.33	0.39	1.29	1.29	1.00
250x100-t1.2-N50-A0	210.98	0.00	1.14	1.13	1.01
250x100-t1.2-N50-MA0.4	204.16	0.37	0.90	0.90	1.00
250x100-t1.2-N50-OA0.4	212.83	0.37	1.01	1.01	1.00
250x100-t1.2-N75-A0	209.28	0.00	1.31	1.33	0.98
250x100-t1.2-N75-MA0.4	209.23	0.39	0.95	0.94	1.01
250x100-t1.2-N75-OA0.4	219.28	0.39	1.02	1.01	1.01
250x100-t1.2-N100-A0	212.87	0.00	1.40	1.38	1.01
250x100-t1.2-N100-MA0.4	232.63	0.39	0.97	0.94	1.03
250x100-t1.2-N100-OA0.4	220.27	0.39	1.08	1.09	0.99
Mean value					1.00
Coefficient of Variation					0.01

3 Parametric study

The developed FE model was used so to complete an extensive study to determine the web bearing capacity of channels without and with circular perforations in web subjected to the ETF load case. The parameters comprise of different lengths of load and reaction plates. The unlipped channels cross-section sizes and the web perforations locations were varied so to investigate the effect of load and reaction plates lengths ratio *(N/h),* web perforations diameter ratio *(a/h)* and web perforations location ratio *(x/h)* on the web bearing capacity of unlipped channels under the ETF load case.

The models of unlipped channel had various depth sizes, with thicknesses (t) between 1.12 to 6.0 mm. Height to thickness (web slenderness) ratios (h/t) were between 148.92 to 232.63. The a/h ratios were 0.2, 0.4, 0.6 and 0.8. The x/h ratios were 0.2, 0.4 and 0.6. The length of load and reaction plates (N) were considered to be 50, 75 and 100 mm. The web bearing capacities of the unlipped channels with no perforations in web were also obtained for each series of models. Hence, the capacity reduction factor (R), which is the ratio of the web bearing capacities for unlipped channels with perforations in web over the web bearing capacities of unlipped channels with no perforations in web, was used as a degrading ratio to quantify the effect of perforations on the

web bearing capacities of unlipped channels. The models have been coded so that the nominal model dimension, the length of the load or reaction plates and Web perforations ratio (A) can be identified in Tables 2 to 3.

In terms of circular web perforation located in between the load and reaction plates, 108 sections were considered to determine the effect of web perforations diameter ratio *(a/h)* as well as load and reaction plates lengths ratio *(N/h)*. Tables 2 to 3 present the web bearing capacities (P_{FEA}) per single web predicted from the FE analyses as well as cross-section dimensions. Fig. 6 demonstrates the effects of the web perforations diameter ratio (a/h) and load and reaction plates lengths ratio (N/h) on the web capacity reduction factors of the C175 section. As can be seen from Fig. 6(a), the reduction factor decreases as the web perforations diameter ratio *(a/h)* increases from the ratio of 0.2 to the ratio of 0.8. Also, it is clear from Fig. 6(b) that the reduction factor is not sensitive to the load and reaction plates length ratio *(N/h)*.

In terms of circular web perforation located in mid-length of the unlipped channels, 252 sections were modelled and analysed to determine the effects of web perforations diameter ratio *(a/h)* and web perforations location ratio (x/h). The web bearing capacities (P_{FEA}) per single web predicted from the FE analyses as well as cross-section dimensions are presented in Table 2. Fig. 7 demonstrates the effects of the web perforations diameter ratio (a/h) and web perforations location ratio (x/h) on the web capacity reduction factors of the C175 section. It can be deduced, from Fig. 7(a), that the capacity reduction factor decreases as the web perforations diameter ratio *(a/h)* increases from the ratio of 0.2 to the ratio of 0.8. Also, it is evident from Fig. 7(b) that the reduction factor is more sensitive to the location of the perforation in the web and the web perforations location ratio (x/h).

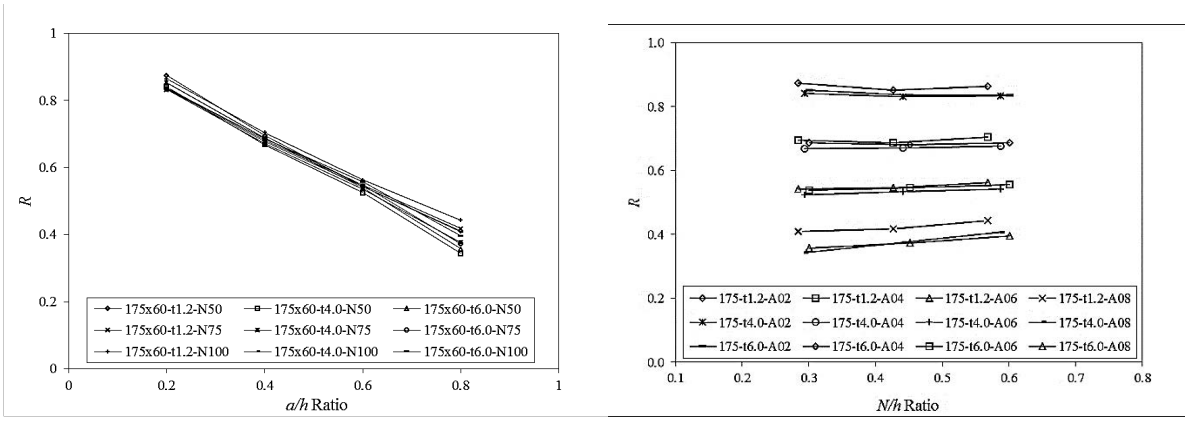

(a) With *a/h* for centred circular web perforation (b) With *N/h* for centred circular web perforation

Figure 6: Reduction factor Variations for C175 section with centred web perforation

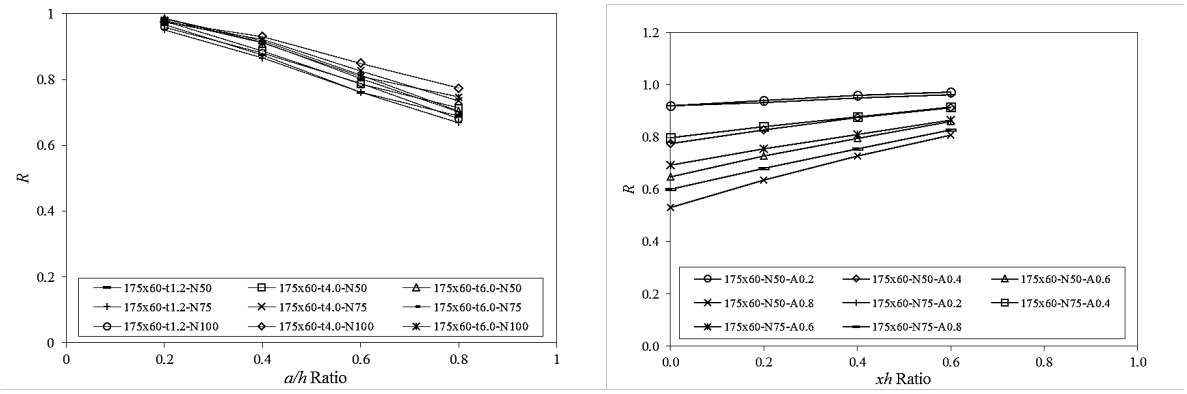

(a) With *a/h* for centred circular web perforation (b) With *x/h* for centred circular web perforation

Figure 7: Reduction factor Variations for C175 section with offset web perforation

Table 2 Section details and web bearing capacities obtained from FEA for parametric study of *a/h* with centred web perforation

Section	Web depth	Flange width	Web thickness	Length of channel	FEA ultimate load per single web, (P_{FEA})				
	(d)	(b_f)	(t)	(L)	(a/h=0)	(a/h=0.2)	(a/h=0.4)	(a/h=0.6)	(a/h=0.8)
	(mm)	(mm)	(mm)	(mm)	(kN)	(kN)	(kN)	(kN)	(kN)
175x60-t1.2-N50	178.54	60.10	1.17	315.17	1.51	1.32	1.05	0.82	0.62
175x60-t4.0-N50	178.54	60.10	4.00	315.17	28.20	23.72	18.84	14.77	9.68
175x60-t6.0-N50	178.54	60.10	6.00	315.17	61.38	52.30	42.18	33.05	21.95
175x60-t1.2-N75	178.15	60.07	1.14	340.00	1.63	1.39	1.12	0.89	0.68
175x60-t4.0-N75	178.15	60.07	4.00	340.00	31.77	26.43	21.31	16.97	11.95
175x60-t6.0-N75	178.15	60.07	6.00	340.00	71.16	59.50	48.46	38.87	26.53
175x60-t1.2-N100	178.34	60.16	1.13	364.67	1.76	1.52	1.24	0.99	0.78
175x60-t4.0-N100	178.34	60.16	4.00	364.67	35.49	29.58	24.05	19.25	14.48
175x60-t6.0-N100	178.34	60.16	6.00	364.67	80.56	67.38	55.30	44.86	31.83
200x75-t1.2-N50	203.54	75.02	1.17	349.67	1.39	1.19	0.95	0.73	0.56
200x75-t4.0-N50	203.54	75.02	4.00	349.67	27.61	23.21	18.63	14.65	9.69
200x75-t6.0-N50	203.54	75.02	6.00	349.67	61.54	52.59	43.04	33.78	21.27
200x75-t1.2-N75	203.56	75.00	1.17	374.67	1.44	1.32	1.07	0.84	0.64
200x75-t4.0-N75	203.56	75.00	4.00	374.67	30.93	25.61	20.34	16.48	11.72
200x75-t6.0-N75	203.56	75.00	6.00	374.67	70.74	54.18	48.49	38.72	25.48
200x75-t1.2-N100	203.76	75.02	1.12	399.33	1.51	1.30	1.06	0.84	0.66
200x75-t4.0-N100	203.76	75.02	4.00	399.33	33.82	28.15	23.04	18.42	13.92
200x75-t6.0-N100	203.76	75.02	6.00	399.33	78.83	65.83	54.55	43.68	30.54
250x100-t1.2-N50	253.47	100.02	1.19	424.33	1.14	0.97	0.76	0.59	0.44
250x100-t4.0-N50	253.47	100.02	4.00	424.33	25.54	21.39	17.12	13.44	9.00
250x100-t6.0-N50	253.47	100.02	6.00	424.33	59.42	50.80	41.12	32.44	18.91
250x100-t1.2-N75	253.54	100.00	1.20	449.50	1.31	1.05	0.83	0.65	0.49
250x100-t4.0-N75	253.54	100.00	4.00	449.50	28.46	23.54	18.90	15.11	10.70
250x100-t6.00-N75	253.54	100.00	6.00	449.50	67.83	56.80	46.11	36.62	22.48
250x100-t1.2-N100	253.59	100.02	1.18	474.50	1.40	1.20	0.96	0.75	0.58
250x100-t4.0-N100	253.59	100.02	4.00	474.50	30.93	25.48	20.57	16.57	12.34
250x100-t6.0-N100	253.59	100.02	6.00	474.50	74.33	62.10	50.45	40.34	26.28

Table 3 Section details and web bearing capacities obtained from FEA for parametric study of *x/h* with offset web perforation

Section	Web depth (d) (mm)	Flange width (b_f) (mm)	Web thickness (t) (mm)	Length of channel (L) (mm)	FEA ultimate load per single web, (P_{FEA}) (x/h=0) (kN)	(x/h=0.2) (kN)	(x/h=0.4) (kN)	(x/h=0.6) (kN)
175x60-t1.2-N50-A0	178.54	60.10	1.17	315.17	1.51	1.51	1.51	1.51
175x60-t1.2-N50-A0.2	178.54	60.10	1.17	315.17	1.39	1.42	1.45	1.47
175x60-t1.2-N50-A0.4	178.54	60.10	1.17	315.17	1.17	1.25	1.32	1.38
175x60-t1.2-N50-A0.6	178.54	60.10	1.17	315.17	0.98	1.10	1.20	1.30
175x60-t1.2-N50-A0.8	178.54	60.10	1.17	315.17	0.80	0.96	1.10	1.22
175x60-t1.2-N75-A0	178.15	60.07	1.14	340.00	1.63	1.63	1.63	1.63
175x60-t1.2-N75-A0.2	178.15	60.07	1.14	340.00	1.50	1.52	1.55	1.57
175x60-t1.2-N75-A0.4	178.15	60.07	1.14	340.00	1.30	1.37	1.43	1.49
175x60-t1.2-N75-A0.6	178.15	60.07	1.14	340.00	1.13	1.23	1.32	1.41
175x60-t1.2-N75-A0.8	178.15	60.07	1.14	340.00	0.98	1.11	1.23	1.35
175x60-t1.2-N100-A0	178.34	60.16	1.13	364.67	1.76	1.76	1.76	1.76
175x60-t1.2-N100-A0.2	178.34	60.16	1.13	364.67	1.65	1.67	1.69	1.72
175x60-t1.2-N100-A0.4	178.34	60.16	1.13	364.67	1.47	1.53	1.59	1.64
175x60-t1.2-N100-A0.6	178.34	60.16	1.13	364.67	1.33	1.41	1.50	1.57
175x60-t1.2-N100-A0.8	178.34	60.16	1.13	364.67	1.17	1.30	1.42	1.52
200x75-t1.2-N50-A0	203.54	75.02	1.17	349.67	1.39	1.39	1.39	1.39
200x75-t1.2-N50-A0.2	203.54	75.02	1.17	349.67	1.24	1.27	1.29	1.32
200x75-t1.2-N50-A0.4	203.54	75.02	1.17	349.67	1.04	1.11	1.17	1.23
200x75-t1.2-N50-A0.6	203.54	75.02	1.17	349.67	0.86	0.96	1.07	1.16
200x75-t1.2-N50-A0.8	203.54	75.02	1.17	349.67	0.70	0.84	0.97	1.09
200x75-t1.2-N75-A0	203.56	75.00	1.17	374.67	1.44	1.44	1.44	1.44
200x75-t1.2-N75-A0.2	203.56	75.00	1.17	374.67	1.41	1.43	1.46	1.48
200x75-t1.2-N75-A0.4	203.56	75.00	1.17	374.67	1.21	1.27	1.34	1.40
200x75-t1.2-N75-A0.6	203.56	75.00	1.17	374.67	1.04	1.14	1.24	1.32
200x75-t1.2-N75-A0.8	203.56	75.00	1.17	374.67	0.89	1.03	1.15	1.26
200x75-t1.2-N100-A0	203.76	75.02	1.12	399.33	1.51	1.51	1.51	1.51
200x75-t1.2-N100-A0.2	203.76	75.02	1.12	399.33	1.43	1.45	1.47	1.49
200x75-t1.2-N100-A0.4	203.76	75.02	1.12	399.33	1.23	1.29	1.36	1.42
200x75-t1.2-N100-A0.6	203.76	75.02	1.12	399.33	1.08	1.17	1.26	1.34
200x75-t1.2-N100-A0.8	203.76	75.02	1.12	399.33	0.96	1.08	1.18	1.29
250x100-t1.2-N50-A0	253.47	100.02	1.19	424.33	1.14	1.14	1.14	1.14
250x100-t1.2-N50-A0.2	253.47	100.02	1.19	424.33	1.01	1.03	1.05	1.07
250x100-t1.2-N50-A0.4	253.47	100.02	1.19	424.33	0.83	0.89	0.94	1.00
250x100-t1.2-N50-A0.6	253.47	100.02	1.19	424.33	0.67	0.77	0.85	0.93
250x100-t1.2-N50-A0.8	253.47	100.02	1.19	424.33	0.63	0.68	0.74	0.84
250x100-t1.2-N75-A0	253.54	100.00	1.20	449.50	1.31	1.31	1.31	1.31
250x100-t1.2-N75-A0.2	253.54	100.00	1.20	449.50	1.10	1.13	1.15	1.17
250x100-t1.2-N75-A0.4	253.54	100.00	1.20	449.50	0.94	0.99	1.07	1.09
250x100-t1.2-N75-A0.6	253.54	100.00	1.20	449.50	0.78	0.87	0.96	1.03
250x100-t1.2-N75-A0.8	253.54	100.00	1.20	449.50	0.68	0.77	0.88	0.97
250x100-t1.2-N100-A0	253.54	100.00	1.20	449.50	1.40	1.40	1.40	1.40
250x100-t1.2-N100-A0.2	253.59	100.02	1.18	474.50	1.27	1.30	1.32	1.34
250x100-t1.2-N100-A0.4	253.59	100.02	1.18	474.50	1.10	1.16	1.22	1.26
250x100-t1.2-N100-A0.6	253.59	100.02	1.18	474.50	0.95	1.04	1.13	1.19
250x100-t1.2-N100-A0.8	253.59	100.02	1.18	474.50	0.82	0.94	1.05	1.14

4 Design comparisons for cold-formed ferritic stainless steel unlipped channels with web perforations

As noted previously, the existing cold-formed standards for design of stainless steel structures are not providing design predictions for determining the web bearing capacity of ferritic stainless steel channels with perforations in web subjected to ETF load case, where the perforation is located either in one end of the unlipped channels in between the load and reaction plates or in mid-length of the channels. However, as seen in laboratory and numerical studies, the web bearing capacities for unlipped channels without perforations in web can be compared to results predicted from the aforementioned standards.

The web bearing capacity obtained from laboratory and numerical studies is compared with results predicted from design standards for the unlipped channels subjected to the ETF load case. In the Eurocode 3 (EN 1993-1-4) comparison, the mean ratio of the laboratory and numerical results over the results predicted from the EN 1993-1-4 standard is 0.96, giving a coefficient of variation of COV=0.19. From the Australian standard (AS/NZS 4673) as well as American specification (SEI/ASCE 8-02) comparisons, the mean ratios are 0.87 and 0.86, with different coefficients of variation of COV=0.27 and COV=0.19, respectively.

It is evident that the Australian standard (AS/NZS 4673) and American specification (SEI/ASCE 8-02) have a more unconservative approach towards predicting the web bearing capacities, in comparison to the Euro standard (EN 1993-1-4). A comparison of the obtained values from the mentioned standards with the results from laboratory and numerical studies shows that capacity predictions from the SEI/ASCE 8-02 specification are 14% higher when compared to the laboratory and numerical failure loads. The current web bearing designs are unconservative and unreliable for cold-formed ferritic stainless steel unlipped channels, having no perforations in web under the ETF load case.

A study by Yousefi et al. (2017c) recommends equations for calculating the capacity reduction factors induced by perforations in web of lipped cold-formed stainless steel channels where the perforations were at the centre of the load and reaction plates or at an offset location. The web bearing capacity reduction factors predicted in Yousefi et al. (2017c) were compared with the capacity reduction factors obtained from laboratory and numerical results.

The capacity reductions factors recommended by Yousefi et al. (2017c) are as follows:

Web perforation in centred location: (3)

$$R_Y = 0.97 - 0.62(\frac{a}{h}) + 0.04(\frac{N}{h}) \leq 1$$

Web perforation in offset location: (4)

$$R_Y = 0.94 - 0.03(\frac{a}{h}) + 0.04(\frac{x}{h}) \leq 1$$

where the limitations for the two above equations are a/h ≤ 0.8, N/h ≤ 1.15, h/t ≤ 157.68, N/t ≤ 120.97 and θ =90º.

The capacity reduction factors obtained from this study are compared with those recommended by Yousefi et al. (2017c) for lipped channels with centred and offset web perforations in Table 4. It is clear that, the equations proposed for lipped channels are unconservative, as well as unreliable, for the unlipped channels; having either centred or offset perforations in web. The mean comparison ratio for both centred and offset perforations is Pm=0.89 having coefficients of variation of COV=0.09 and COV=0.11 for centred and offset perforations. Therefore, the recommended design equations for lipped channels are unconservative for unlipped cold-formed ferritic stainless steel channels by as much as 11% as well as unreliable to use. This can be explained by the fact that the equations recommended by Yousefi et al. (2017c) were applicable for only lipped channels having different stainless steel grades.

5 Proposed capacity reduction factors and comparison with laboratory and numerical analyses results

As shown in Tables 2 to 3, the ultimate bearing capacity increases as the circular web perforations diameter decreases. Also, as the distance from the edge of the load and reaction plates increases, the ultimate capacity increases as well. As expected, it is also evident from Tables 2 to 3 that the ultimate web bearing capacities are affected by the length of the load and reaction plates. It increases as the length of the load and reaction plates increases. Evaluating results from the laboratory and numerical analyses, it is shown that web perforations diameter ratio *(a/h),* load and reaction plates lengths ratio *(N/h),* and web perforations location ratio (*x/h)* can be the main factors affecting the web bearing capacity of the unlipped channels having web perforations under the ETF load case. Hence, according to both the numerical and the laboratory results obtained from this study and upon performing bivariate regression analysis, two bearing capacity reduction factor equations (R_D) are proposed for the unlipped channels with centred and offset web perforations under the ETF load case.

Web perforation in centred location:

$$R_D = 0.97 - 0.76(\frac{a}{h}) + 0.06(\frac{N}{h}) \leq 1 \quad (5)$$

Web perforation in offset location:

$$R_D = 0.96 - 0.41(\frac{a}{h}) + 0.25(\frac{x}{h}) \leq 1 \quad (6)$$

where the limitations for the two above equations are $a/h \leq 0.8$, $N/h \leq 0.61$, $h/t \leq 200$, $N/t \leq 90.09$ and $\theta = 90^o$.

The calculated capacity reduction factors from the proposed Eqs. (5) and (6), are compared to the obtained capacity reduction factor values from the numerical and laboratory results, as depicted versus the web perforations diameter ratio *(a/h)* and web slenderness ratio (*h/t*) in Figs. 8 and 9. In order to show the reliability of the proposed reduction factors, a summary of statistical values for reliability analysis is presented in Tables 5 and 10. The proposed equations are evidently conservative and match well with the results for unlipped channels with centred and offset perforations in web.

In terms of centred web perforations, it is evident from Table 5 that the mean of the obtained capacity reduction factor values from the numerical and the laboratory analyses results over the results from proposed capacity reduction factor is 1.00, having the coefficient of variation of COV=0.05 and having the corresponding reliability index value of β=2.84. In regards to offset web perforations, it is clear from Table 5 that the mean ratio of the obtained capacity reduction factor values from the numerical and the laboratory analyses results over the results from proposed capacity reduction factor is also 1.00, having the coefficient of variation of COV=0.06 and having the reliability index value of β=2.74. Thus, the equations proposed for ferritic stainless steel unlipped channels having centred or offset perforations in web can well predict the web bearing capacity reduction factor of such chan

Table 4 Comparison of web bearing capacity reduction factor with reduction factors equations proposed by Yousefi *et al.* (2017c)

Specimen	Failure load without web openings $P_{(A0)}$	Failure load with web openings $P_{(Web\ opening)}$		Reduction factor $R=P_{(Web\ opening)}/P_{(A0)}$		Factored resistance *(Eq. 3)*	Factored resistance *(Eq. 4)*	Comparison with factor resistance from Yousefi *et al.* R/R_{Lipped}	
	(kN)	Centred	Offset	Centred	Offset	Centred	Offset	Centred	Offset
175x60-t1.2-N50-A0.2	1.51	1.32	1.46	0.87	0.97	0.86	0.95	1.02	1.02
175x60-t1.2-N50-A0.4	1.51	1.05	1.32	0.70	0.87	0.73	0.94	0.95	0.93
175x60-t1.2-N50-A0.6	1.51	0.82	1.15	0.54	0.76	0.61	0.93	0.89	0.82
175x60-t1.2-N50-A0.8	1.51	0.62	1.04	0.41	0.69	0.49	0.93	0.85	0.74
200x75-t4.0-N75-A0.2	30.93	25.61	29.06	0.83	0.94	0.86	0.95	0.96	0.99
200x75-t4.0-N75-A0.4	30.93	20.34	27.21	0.66	0.88	0.74	0.94	0.89	0.94
200x75-t4.0-N75-A0.6	30.93	16.48	25.14	0.53	0.81	0.61	0.93	0.87	0.87
200x75-t4.0-N75-A0.8	30.93	11.72	22.64	0.38	0.73	0.49	0.93	0.77	0.79
250x100-t6.0-N100-A0.2	74.33	62.1	72.62	0.84	0.98	0.86	0.95	0.97	1.03
250x100-t6.0-N100-A0.4	74.33	50.45	67.79	0.68	0.91	0.74	0.94	0.92	0.97
250x100-t6.0-N100-A0.6	74.33	40.34	59.98	0.54	0.81	0.61	0.93	0.88	0.86
250x100-t6.0-N100-A0.8	74.33	26.28	52.25	0.35	0.70	0.49	0.93	0.72	0.76
Mean value, (P_m)								0.89	0.89
CoV								0.09	0.11
Reliability index, (β)								1.96	1.90
Resistance factor, (ϕ)								0.85	0.85

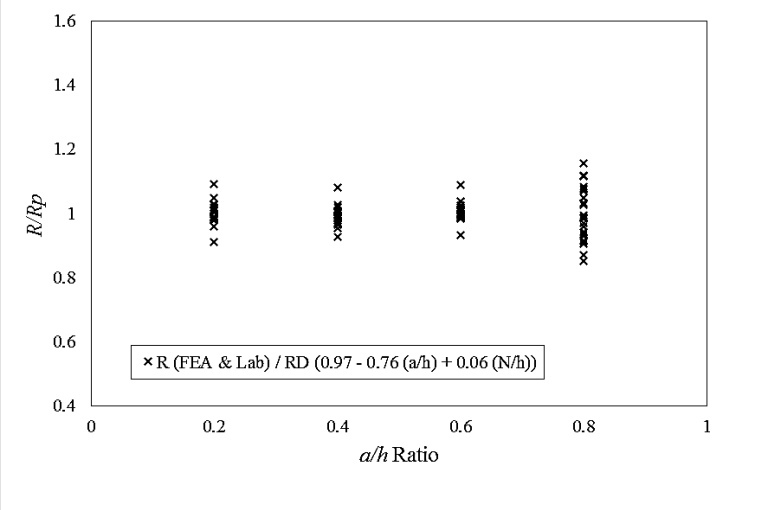

Figure 8: Capacity reduction factor comparison for centred web perforation

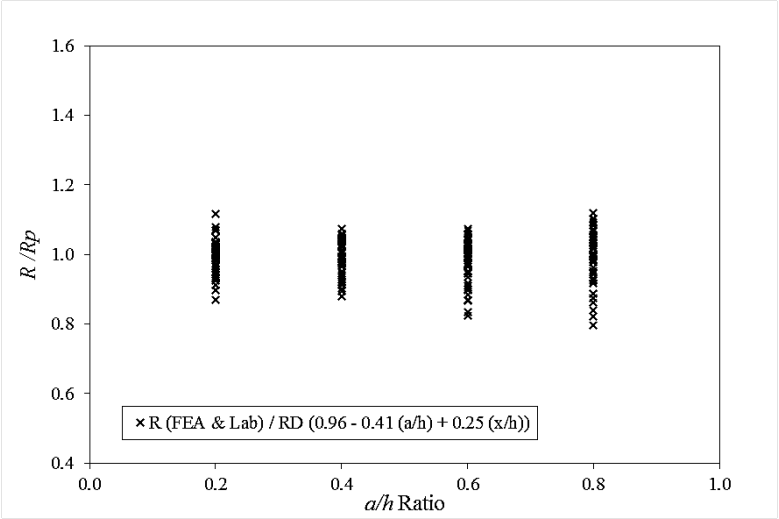

Figure 9: Capacity reduction factor comparison for offset web perforation

Table 5: Statistical analysis of capacity reduction factor

Statistical parameters	Reduction factor comparison $R_{(FEA)} / R_p$	
	Centred perforation	Offset perforation
Number of data	108	252
Mean, P_m	1.00	1.00
Coefficient of variation, V_p	0.05	0.06
Reliability index, β	2.84	2.74
Resistance factor, ϕ	0.85	0.85

6 Conclusions

This paper has presented laboratory and numerical evaluation on the bearing capacity of unlipped cold-formed ferritic stainless steel channels subject to end-two-flange (ETF) load case. The laboratory programme comprised unlipped channels without and with circular perforations in web, located either at one end of the unlipped sections in between the load and reaction plates (centred), or in mid-length of the sections (offset). A finite element (FE) model was then developed using the general application FE software ABAQUS (2014) and verified against the laboratory result, showing a good prediction for web bearing capacity. The developed FE model was then used in order to carry out an extensive study to determine the web bearing capacity of channels without and with circular perforations in web subjected to the ETF load case. The parameters comprised different lengths of load and reaction plates; the unlipped channels cross-section sizes and the web perforations locations were varied to investigate the effect of load and reaction plates lengths ratio *(N/h),* web perforations diameter ratio *(a/h)* and web perforations location ratio (*x/h)* on the web bearing capacity of unlipped channels under the ETF load case. Capacity reduction factors from this study were also compared against Yousefi *et al.* (2017c) for lipped stainless steel channels. These reduction factor equations were demonstrated to be unconservative and unreliable for unlipped cold-formed ferritic stainless steel channels by as much as 11%. Using both laboratory and numerical results, new web bearing capacity equations have been proposed for cold-formed ferritic stainless steel unlipped channels with and without circular perforations in web subject to ETF load case. It is demonstrated that the proposed equations are suitable and conservative for use. From the reliability analysis, the proposed equations are shown to be reliable when compared against both laboratory and numerical results.

References

ABAQUS version 6.14-2 [Computer software]. Dassault Systemes, Waltham, MA, 2014.

American Iron and Steel Institute Specification (AISI). (2016). "North American Specification for the Design of Cold-Formed Steel Structural Members."AISI S100-16, Washington, D.C.

American Society of Civil Engineers (ASCE). (2010). "Minimum design loads for buildings and other structures." SEI/ASCE 7-10, New York.

American Society of Civil Engineers (ASCE). (2002). "Specification for the design of cold-formed stainless steel structural members." SEI/ASCE 8-02, Reston,Va.

Australian/New Zealand Standard (AS/NZS). (2001). "Cold-formed stainless steel structures." *AS/NZS 4673:2001*, Standards Australia, Sydney, Australia.

Cashell, K. A., and Baddoo, N. R. (2014). "Ferritic stainless steels in structural applications." *Thin-Wall. Struct.*, 83, 169-181.

CEN (European Committee for Standardization. (2006). "Design of steel structures: Part 1.4: General rules: Supplementary rules for stainless steels." *Eurocode 3, EN 1993-1-4,* Brussel, Belgium.

CEN (European Committee for Standardization. (2006). "General rules: Supplementary rules for cold-formed members and sheeting." *Eurocode 3, EN 1993-1-3,* Brussel, Belgium.

ISO E. 6892-1. (2009). "Metallic Materials: Tensile Testing: Part 1: Method of Test at Room Temperature" *ISO E. 6892-1*, International Standard, Geneva.

Korvink, S. A., Van den Berg, G. J., and Van der Merwe, P. (1995). "Web crippling of stainless steel cold-formed beams." *J. Constr. Steel Res.*, 34(2-3), 225-248.

Korvink, S. A., Van den Berg, G. J. (1994). "Web crippling of stainless steel cold-formed beams." *Proc., 12th Int. Specialty Conf. on Cold-Formed Steel Structures, University of Missouri-Rolla, St. Louis, 551-569.*

Lawson, R. M., Basta, A., and Uzzaman, A. (2015). "Design of stainless steel sections with circular openings in shear." *J. Constr. Steel Res.*, 112, 228-241.

Lian, Y., Uzzaman, A., Lim, J. B. P., Abdelal, G., Nash, D., and Young, B. (2017). "Web crippling behaviour of cold-formed steel channel sections with web holes subjected to Interior-one-flange loading condition-part I: experimental and numerical investigation." *Thin-Wall. Struct.*, 111, 103-112.

Lian, Y., Uzzaman, A., Lim, J. B. P., Abdelal, G., Nash, D., and Young, B. (2016). "Effect of web holes on web crippling strength of cold-formed steel channel sections under end-one-flange loading condition–Part I: Tests and finite element analysis." *Thin-Wall. Struct.*, 107, 443-452.

Li, H. T., and Young, B. (2017a). "Cold-formed ferritic stainless steel tubular structural members subjected to concentrated bearing loads." *Eng. Struct.*, 145, 392-405.

Li, H. T., and Young, B. (2017b). "Tests of cold-formed high strength steel tubular sections undergoing web crippling." *Eng. Struct.*, 141, 571-583.

Mohammadjani, C., Yousefi, A. M., Cai, S. Q., Clifton, G. C., and Lim, J. B. P. (2017). "Strength and stiffness of cold-formed steel portal frame joints using quasi-static finite element analysis." *Steel Compos. Struct.*, Int. J., *25*(6), 727-734.

Rezvani, F. H., Yousefi, A. M., Ronagh, H. R. (2015). "Effect of span length on progressive collapse behaviour of steel moment resisting frames". *Structures,* 3, 81-89.

Uzzaman, A., Lim, J. B. P., Nash, D., Rhodes, J., and Young, B. (2012). "Web crippling behaviour of cold-formed steel channel sections with offset web holes subjected to interior-two-flange loading." *Thin-Wall. Struct.*, 50, 76-86.

Uzzaman, A., Lim, J. B. P., Nash, D., Rhodes, J., and Young, B. (2013). "Effect of offset web holes on web crippling strength of cold-formed steel channel sections under end-two-flange loading condition." *Thin-Wall. Struct.*, 65, 34-48.

Young, B., and Hancock, G. J. (2001). "Design of cold-formed channels subjected to web crippling." *J. Struct. Eng.*, 10.1061/(ASCE)0733-9445(2001)127:10(1137), 1137-1144.

Yousefi, A. M., Lim, J. B. P., and Clifton, G. C. (2018). Web crippling behaviour of unlipped cold-formed ferritic stainless steel channels subject to one-flange loading, *J. Struct. Eng.*, DOI: 10.1061/(ASCE)ST.1943-541X.0002118.

Yousefi, A. M., Lim, J. B. P., Uzzaman, A., Lian, Y., Clifton, G. C., and Young, B. (2017a). "Design of cold-formed stainless steel lipped channel sections with web openings subjected to web crippling under end-one-flange loading condition." *Adv. Struct. Eng.*, 20(7), 1024-1045.

Yousefi, A. M., Uzzaman, A., Lim, J. B. P., Clifton, G. C., and Young, B. (2017b). "Numerical investigation of web crippling strength in cold-formed stainless steel lipped channels with web openings subjected to interior-two-flange loading condition." *Steel Compos. Struct.*, Int. J., *23*(4), 363-383.

Yousefi, A. M., Uzzaman, A., Lim, J. B. P., Clifton, G. C., and Young, B. (2017c). "Web crippling strength of cold-formed stainless-steel lipped channels with web perforations under end-two-flange loading." *Adv. Struct. Eng.*, 20(12), 1845-1863.

Yousefi, A. M., Lim, J. B. P., and Clifton, G. C. (2017d). "Cold-formed ferritic stainless steel unlipped channels with web openings subjected to web crippling under interior-two-flange loading condition-part I: Tests and finite element model validation." *Thin-Wall. Struct.,* 116, 333-341.

Yousefi, A. M., Lim, J. B. P., and Clifton, G. C. (2017e). "Cold-formed ferritic stainless steel unlipped channels with web openings subjected to web crippling under interior-two-flange loading condition-part II: Parametric Study and design equations." *Thin-Wall. Struct.,* 116, 342-356.

Yousefi, A. M., Lim, J. B. P., and Clifton, G. C. (2017f). "Web bearing capacity of ulipped cold-formed ferritic stainless steel channels with perforated web subject to end-two-flange (ETF) loading." *Eng. Struct*., 152, 804-818.

Yousefi, A. M., Lim, J. B. P., Uzzaman, A., Lian, Y., Clifton, G. C., and Young, B. (2016a). "Web crippling strength of cold-formed stainless steel lipped channel-sections with web openings subjected to interior-one-flange loading condition." *Steel Compos. Struct.*, Int. J., *21*(3), 629-659.

Yousefi, A. M., Lim, J. B. P., Uzzaman, A., Lian, Y., Clifton, G. C., and Young, B. (2016b). " Web Crippling Strength of Cold-Formed Duplex Stainless Steel Lipped Channel-Sections with Web Openings Subjected to Interior-One-Flange Loading Condition."*Proc., Wei-Wen Yu Int. Specialty Conf. on Cold-Formed Steel Structures,* Univ. of Missouri-Rolla, Missouri, 313-324.

Yousefi, A. M., Hosseini M., Fanaie, N. (2014). "Vulnerability Assessment of Progressive Collapse of Steel Moment Resistant Frames." *Trends in Applied Sciences Research, 9 450-460.*

Zhou, F., and Young, B. (2013). "Web crippling behaviour of cold-formed duplex stainless steel tubular sections at elevated temperatures." *Eng. Struct.*, 57, 51-62.

Zhou, F., and Young, B. (2010). "Web crippling of aluminium tubes with perforated webs." *Eng. Struct.*, 32(5), 1397-1410.

Zhou, F., and Young, B. (2007a). "Cold-formed high-strength stainless steel tubular sections subjected to web crippling." *J. Struct. Eng.,* 10.1061/(ASCE)0733-9445(2007)133:3(368), 368-377.

Zhou, F., and Young, B. (2007b). "Experimental and numerical investigations of cold-formed stainless steel tubular sections subjected to concentrated bearing load." J. Constr. Steel Res., 63(11), 1452-1466.

Zhou, F., and Young, B. (2006). "Cold-formed stainless steel sections subjected to web crippling." J. Struct. Eng., 10.1061/(ASCE)0733-9445(2006)132:1(134), 134-144